ORIGINAL ARTICLE

Mast Cells Play a Key Role in Host Defense against Herpes Simplex Virus Infection through TNF-α and IL-6 Production

Rui Aoki[1], Tatsuyoshi Kawamura[1], Fumi Goshima[2], Youichi Ogawa[1], Susumu Nakae[3], Atsuhito Nakao[4], Kohji Moriishi[5], Yukihiro Nishiyama[2] and Shinji Shimada[1]

The essential contribution of mast cells (MCs) to bacterial host defense has been well established; however, little is known about their role in viral infections *in vivo*. Here, we found that intradermal injection with herpes simplex virus 2 (HSV-2) into MC-deficient $Kit^{W/Wv}$ mice led to increased clinical severity and mortality with elevated virus titers in HSV-infected skins. *Ex vivo* HSV-specific tetramer staining assay demonstrated that MC deficiency did not affect the frequency of HSV-specific cytotoxic T lymphocytes (CTLs) in draining lymph nodes. Moreover, the high mortality in $Kit^{W/W\text{-}v}$ mice was completely reversed by intradermal reconstitution with bone marrow–derived MCs (BMMCs) from wild-type, but not $TNF^{-/-}$ or IL-$6^{-/-}$ mice, indicating that MCs or, more specifically, MC-derived tumor necrosis factor (TNF) and IL-6 can protect mice from HSV-induced mortality. However, HSV did not directly induce TNF-α or IL-6 production by BMMCs; supernatants from HSV-infected keratinocytes induced the production of these cytokines by BMMCs without degranulation. Furthermore, IL-33 expression was induced in HSV-infected keratinocytes, and blocking the IL-33 receptor T1/ST2 on BMMCs significantly reduced TNF-α and IL-6 production by BMMCs. These results indicate the involvement of MCs in host defense at HSV-infected sites through TNF-α and IL-6 production, which is induced by keratinocyte-derived IL-33.

Journal of Investigative Dermatology (2013) **133,** 2170–2179; doi:10.1038/jid.2013.150; published online 9 May 2013

INTRODUCTION

Mast cells (MCs) are not only effector cells in allergic responses but are also initiator and regulator cells in both innate and adaptive immune responses (Galli *et al.*, 2005). They are widely distributed throughout the body, in particular at host/environmental interfaces such as the skin and airways, where they preferentially localize around nerves and blood vessels (Galli *et al.*, 2005). They can therefore act as important sentinels for the immune system and control effective innate responses against invading pathogens by releasing various mediators, including a diverse array of cytokines, chemokines, and lipid mediators (Metz and Maurer, 2007; Abraham and St John, 2010).

The development of MC-deficient mouse models allows testing of MC contribution to biological responses of interest, both through the analysis of experimental outcomes in MC-deficient mice and those in mice in which MC deficiency has been selectively repaired by local engraftment (Galli *et al.*, 2005; Metz and Maurer, 2007). Using this so-called "MC knock-in mouse" model, several studies have demonstrated that MCs are critical effector cells in eliciting protective immune responses against bacteria, and that MC-derived tumor necrosis factor-α (TNF-α) is largely responsible for bacterial clearance by inducing neutrophil recruitment into sites of infection (Echtenacher *et al.*, 1996; Malaviya *et al.*, 1996). For the many MCs located proximal to blood vessels, the release of factors such as other cytokines, histamine, proteases, and chemokines also contributes to increased local vascular permeability and recruitment of other participants in the inflammatory response at the site of infection (Abraham and St John, 2010).

In contrast to the well-established contributions of MCs to host defense against bacteria, the function of MCs in antiviral immunity has not been well defined. We and others have previously reported that Toll-like receptor 3 (TLR3)-, TLR7-, and TLR9-mediated activation of MCs can induce selective production of cytokines and chemokines, suggesting that MCs

[1]*Department of Dermatology, Faculty of Medicine, University of Yamanashi, Chuo, Yamanashi, Japan;* [2]*Department of Virology, Nagoya University Graduate School of Medicine, Nagoya, Japan;* [3]*Laboratory of Systems Biology, Center for Experimental Medicine and Systems Biology, Institute of Medical Science, University of Tokyo, Tokyo, Japan;* [4]*Department of Immunology, Faculty of Medicine, University of Yamanashi, Chuo, Yamanashi, Japan and* [5]*Department of Microbiology, Faculty of Medicine, University of Yamanashi, Chuo, Yamanashi, Japan*

Correspondence: Tatsuyoshi Kawamura, Department of Dermatology, Faculty of Medicine, University of Yamanashi, 1110 Shimokato, Chuo, Yamanashi 409-3898, Japan. E-mail: tkawa@yamanashi.ac.jp

Abbreviations: BMMC, bone marrow–derived mast cell; CTL, cytotoxic T lymphocyte; DC, dendritic cell; DLN, draining lymph node; HSV-2, herpes simplex virus-2; MC, mast cell; MOI, multiplicity of infection; NK, natural killer; TNF-α, tumor necrosis factor-α; TLR, Toll-like receptor; WT, wild type

Received 8 November 2012; revised 19 February 2013; accepted 5 March 2013; accepted article preview online 25 March 2013; published online 9 May 2013

are capable of secreting these mediators in response to virus-derived pathogen-associated molecular patterns (Kulka *et al.*, 2004; Matsushima *et al.*, 2004). Indeed, several viruses, including dengue virus and adenovirus, have been shown to activate MCs *in vitro* through TLR3, TLR7, and possibly other mechanisms (Dawicki and Marshall, 2007). Nevertheless, the *in vivo* contribution of MCs to host defense in viral infections is less clear, mainly because suitable mouse models of viral infection have not been tested in the "MC knock-in mouse" model until recently (Metz *et al.*, 2008; Abraham and St John, 2010). However, two very recent studies have revealed the *in vivo* role of MCs in protective immune responses against viral infection using "MC knock-in mouse" model, and demonstrated that natural killer (NK) and NK T-cell recruitment promoted by MCs or MC-derived antimicrobial peptides has a pivotal role in viral clearance during dengue virus or vaccina virus infection, respectively (St John *et al.*, 2011; Wang *et al.*, 2012).

Herpes simplex virus type 2 (HSV-2) is a sexually transmitted pathogen that infects more than 500 million people worldwide and causes most cases of genital herpes (Looker *et al.*, 2008). In cutaneous herpes simplex lesions of humans and in murine models, keratinocytes, dendritic cells (DCs), and infiltrating lymphocytes, especially HSV-specific CD8 T lymphocytes, are known to have a central role in controlling primary and recurrent HSV infections (Simmons and Tscharke, 1992; Chew *et al.*, 2009). Moreover, the important role of other innate immune effectors such as NK cells, NK T cells, plasmacytoid DCs, macrophages, and γδ T lymphocytes has been recently re-emphasized, either in direct immune control or via modulation of adaptive immune responses in HSV infection (Cheng *et al.*, 2000; Chew *et al.*, 2009; Melchjorsen *et al.*, 2009). However, very little *in vitro* and *in vivo* data exist regarding the role of MCs in HSV infections.

Here, we examined the *in vivo* contribution of MCs to the immune responses against HSV using the "MC knock-in mouse" model and demonstrated that MCs were critically involved in host defense at HSV-infected sites through TNF-α and IL-6 production. Our study also suggests an important role for IL-33 derived from HSV-infected keratinocytes as a trigger for the production of these inflammatory cytokines by MCs.

RESULTS

MC-deficient mice exhibit high mortality and local inflammation following cutaneous HSV infection

We first assessed the role of MCs *in vivo* by using a murine model of lethal HSV encephalitis (Corey and Spear, 1986), whereby peripheral infection with HSV involves local replication in the skin, followed by rapid dissemination of the virus via sensory axons, causing zosteriform lesions to spread from the primary inoculation site along the affected dermatomes, and leading to paralysis and death. Using this model, MC-deficient $Kit^{W/W\text{-}v}$ mice and $Kit^{+/+}$ wild-type (WT) mice were injected intradermally with HSV-2 (7.5×10^4 PFU) and were monitored for survival and scored for paralysis and skin lesions. Intriguingly, $Kit^{W/W\text{-}v}$ mice exhibited markedly decreased percent survival when compared with $Kit^{+/+}$ mice (Figure 1a). We also compared clinical severity in these mice by using the experimental autoimmune encephalomyelitis score, which reflects paralysis. The clinical score in $Kit^{W/W\text{-}v}$ mice was significantly higher than that in $Kit^{+/+}$ mice (Figure 1b). We obtained similar findings when we repeated the experiments with MC-deficient $Kit^{W\text{-}sh/W\text{-}sh}$ mice injected intradermally with HSV-2 (Supplementary Figure S1a and b online). As shown in Figure 1c, the zosteriform eruption in the skin lesions of $Kit^{W/W\text{-}v}$ mice appeared at an earlier time point, and exacerbated more rapidly and severely than that of $Kit^{+/+}$ mice. Consistent with these findings, histological examination of the zosteriform lesion in $Kit^{W/W\text{-}v}$ mice revealed increased inflammation and an extended infection area, as demonstrated by HSV glycoprotein D antigen expression in subepithelial tissue, when compared with that in $Kit^{+/+}$ mice, at 3 and 5 days post infection (Figure 1d and e). On the basis of this histopathological observation, we assessed whether MCs contribute to HSV clearance by measuring virus titers in the HSV-infected skins of $Kit^{+/+}$ and $Kit^{W/W\text{-}v}$ mice. The virus titers in $Kit^{W/W\text{-}v}$ mice rapidly increased, reaching maximal levels at day 5, and dropped afterward (Figure 1f). In contrast, the skin lesions of $Kit^{+/+}$ mice contained lower virus titers, which were sustained until day 7. These results suggested that the severe inflammation and mortality observed in $Kit^{W/W\text{-}v}$ mice may be attributed to impaired virus clearance during these early stages of HSV infection, particularly during the first 3 days.

MCs produce TNF-α and IL-6, but not IFN-α, in response to soluble factors released from HSV-infected keratinocytes

The impaired clearance of HSV-2 in the skin lesion of $Kit^{W/W\text{-}v}$ mice was observed during the first 72 hours after infection (Figure 1f), suggesting that MCs are involved in innate immunity, rather than acquired immunity, against HSV-2. In early immune responses in HSV infection, several studies highlight the importance of TNF-α for protection against lethal HSV encephalitis (Rossol-Voth *et al.*, 1991; Lundberg *et al.*, 2007). In addition, TNF-α has been shown to control HSV replication, independent of T and B cells (Feduchi *et al.*, 1989; Heise and Virgin, 1995). Other studies indicated that IL-6 and IFN-α decrease the susceptibility to HSV infection (Murphy *et al.*, 2008; Melchjorsen *et al.*, 2009). Consistent with these findings, we could detect the production of TNF-α, IL-6, and IFN-α at HSV-2 injection sites 72 hours after infection in WT mice (Supplementary Figure S3a online). Therefore, we next assessed whether HSV-2 directly induced cytokine production by BMMCs. However, MCs are resistant to HSV-2 infection (Supplementary Figure S4a online), and HSV-2 exposure did not induce TNF-α and IL-6 production or degranulation by BMMCs (Supplementary Figure S4b–d online).

Because the major cellular targets for HSV-2 were found to be epidermal keratinocytes in the skin lesion of $Kit^{+/+}$ and $Kit^{W/W\text{-}v}$ mice at 3 days after infection Figure 1d), we hypothesized that soluble factors released from HSV-infected keratinocytes may induce the cytokine production by MCs. Strikingly, as shown in Figure 2a and b, the supernatants of HSV-treated keratinocytes, Pam-212, induced significant TNF-α and IL-6 production by BMMCs in a multiplicity of infection (MOI)–dependent manner, whereas they failed to induce

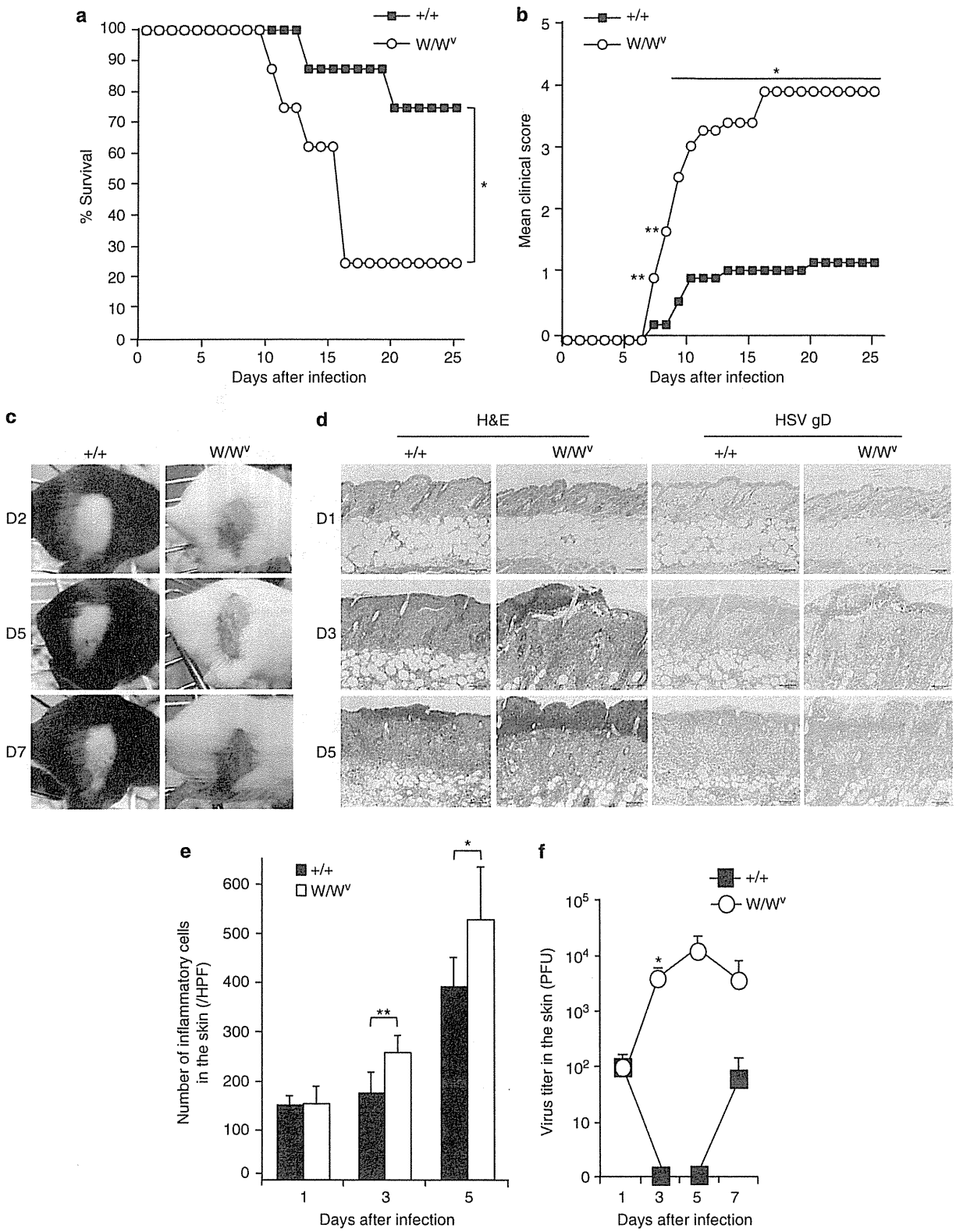
a
+/+
W/W^v
% Survival
Days after infection
b
Mean clinical score
Days after infection
c
+/+
W/W^v
D2
D5
D7
d
H&E
HSV gD
D1
D3
D5
e
Number of inflammatory cells in the skin (/HPF)
Days after infection
f
Virus titer in the skin (PFU)
Days after infection

degranulation in, and IFN-α production by, BMMCs (Figure 2c and d). Notably, *in vitro* HSV infection of keratinocytes did not directly induce the production of these cytokines (Supplementary Figure S3b online). These results imply that MCs may be capable of producing TNF-α and IL-6 in response to cutaneous HSV-2 infection *in vivo* by indirect stimulation via soluble factors derived from HSV-infected keratinocytes. Interestingly, as shown in Supplementary Figure S2a and c online, HSV-2 did not significantly increase MC degranulation in the skin *in vivo*.

MCs, particularly MC-derived TNF-α and IL-6, protect mice from HSV-induced severe mortality

To confirm whether the different responses against cutaneous HSV-2 infection in $Kit^{+/+}$ and $Kit^{W/W\text{-}v}$ mice observed in Figure 1 reflect the lack of MCs in $Kit^{W/W\text{-}v}$ mice rather than other c-Kit-related differences (Galli *et al.*, 2005), we examined $Kit^{W/W\text{-}v}$ mice locally reconstituted with BMMCs derived from $Kit^{+/+}$ mice (WT BMMC→$Kit^{W/W\text{-}v}$). As expected, the decreased survival rate and the severe clinical and lesion score in HSV-infected $Kit^{W/W\text{-}v}$ mice were significantly improved by local reconstitution with MCs, comparable to those in $Kit^{+/+}$ mice (Figure 3a–c). Nevertheless, local reconstitution of $Kit^{W/W\text{-}v}$ mice with BMMCs derived from TNF-deficient mice ($TNF^{-/-}$ BMMC→$Kit^{W/W\text{-}v}$) or IL-6-deficient mice ($IL\text{-}6^{-/-}$ BMMC→$Kit^{W/W\text{-}v}$) did not significantly improve percent survival, clinical score, or lesion score (Figure 3a–c). These results clearly indicate that both MC-produced TNF and IL-6 critically contribute to protective antiviral responses to HSV-2 *in vivo*.

IL-33 derived from HSV-2-treated keratinocytes can induce cytokine production by MCs

Next, we explored which soluble factors released by HSV-2-treated keratinocytes induce TNF-α and IL-6 production by MCs. Recent studies have highlighted the important roles of IL-33 as an "alarmin" in innate immune responses, as IL-33, as a key product of epithelial barrier tissues such as the skin, can be released into the extracellular space after epithelial cell damage during infection or trauma, and it functions as an alarmin to alert the immune system (Moussion *et al.*, 2008; Luthi *et al.*, 2009). It is notable that IL-33 has recently been shown to be upregulated in the lung during viral infection with influenza virus and spleen during infection with lymphocytic choriomeningitis virus (Chang *et al.*, 2011; Bonilla *et al.*, 2012). In line with these findings, we found that increased IL-33 expression was selectively detected on damaged or degenerating Pam-212 cells after *in vitro* HSV-2 exposure, and the frequency of IL-33-expressing cells was increased in an MOI-dependent manner (Figure 4a). In addition, we found a significant increase in IL-33 production by HSV-infected Pam-212 cells (Figure 4a). Importantly, we found that IL-6 and TNF-α production by BMMCs in response to the supernatants from HSV-2-treated Pam-212 cells was significantly and most effectively reduced by blockade of the IL-33 receptor using the T1/ST2 antibody (Figure 4b). Conversely, IL-6 production was not affected by neutralization of other cytokines including IL-1α, IFN-β, and thymic stromal lymphopoietin (Supplementary Figure S5 online). Furthermore, we found that IL-33 stimulates the production of TNF-α and IL-6 by BMMCs in a dose-dependent manner (Figure 4c), without inducing degranulation (data not shown). On the basis of these results,

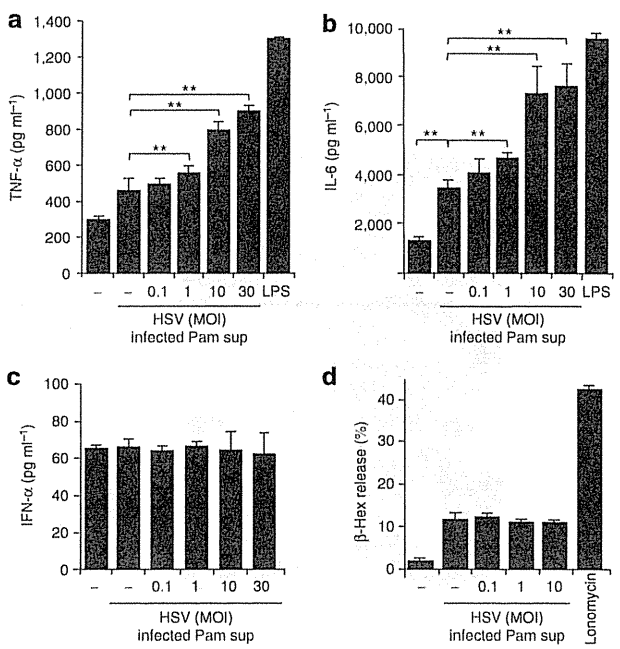

Figure 2. Supernatants of herpes simplex virus 2 (HSV)–infected keratinocytes induce tumor necrosis factor-α (TNF-α) and IL-6, but not IFN-α, production by bone marrow–derived mast cells (BMMCs). BMMCs were stimulated with culture supernatants (sup) from Pam-212 cells treated with or without HSV at multiplicities of infection (MOIs) of 0.1, 1, 10, or 30, or with lipopolysaccharide (LPS; 10 ng ml^{-1}) as a positive control for 24 hours, and assessed for (**a**) TNF-α, (**b**) IL-6, and (**c**) IFN-α production by ELISA. (**d**) β-Hexosaminidase (β-Hex) assay of BMMCs at 1 hour after stimulation with the culture supernatants from Pam-212 cells treated with or without HSV at MOIs of 0.1, 1, or 10 for 24 hours, or with ionomycin (1 μM) for 10 minutes as a positive control. $^{**}P<0.01$ versus results for untreated Pam-212 cells. Data are representative of three independent experiments, showing the means ($n=3$) ± SD.

Figure 1. Mast cell (MC)-deficient mice exhibit increased clinical severity and mortality following cutaneous herpes simplex virus 2 (HSV-2) infection. MC-deficient C57BL/6-$Kit^{W/W\text{-}v}$ mice (white circles) and the corresponding wild-type (WT) C57BL/6-$Kit^{+/+}$ mice (black squares) ($n=8$) were injected intradermally with HSV-2 186 strain (7.5×10^4 PFU) on the right back. (**a**) Survival rates, (**b**) mean clinical scores, (**c**, **d**) representative clinical photos and cross-sections stained with anti-HSV antibody (Ab) or by hematoxylin and eosin (H&E) staining of HSV-infected skins (original magnification × 200, scale bar = 100 μm), (**e**) quantification of the cell infiltrate in **d** throughout 10 high-power fields (HPFs) of view, and (**f**) HSV titers in the skin ($n=3$) measured in plaque assays at the indicated time points after HSV-2 inoculation are shown. gD, glycoprotein D. The results of $Kit^{+/+}$ mice at days 3 and 5 were below the limit of detection. $^{*}P<0.05$ and $^{**}P<0.01$ versus the corresponding WT mice. Data are representative of at least three independent experiments with similar results, showing the means ($n=3$) ± SD.

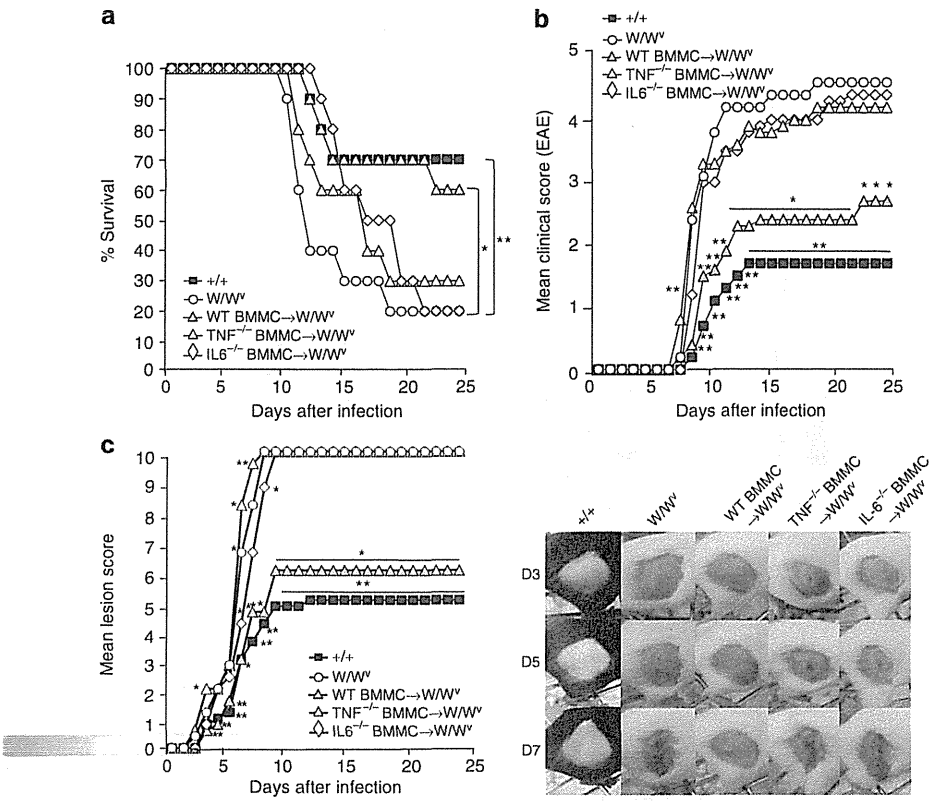

Figure 3. Reconstitution with bone marrow–derived mast cells (BMMCs) derived from wild-type (WT) but not TNF$^{-/-}$ or IL-6$^{-/-}$ mice prevents mortality in Kit$^{W/W\text{-}v}$ mice. (**a**) Survival rates, (**b**) clinical (experimental autoimmune encephalomyelitis (EAE)) scores, (**c**) lesion scores, and representative clinical photographs of skin lesions of Kit$^{W/W\text{-}v}$ mice (white circles), WT Kit$^{+/+}$ mice (black squares), WT BMMC-reconstituted Kit$^{W/W\text{-}v}$ mice (gray circles), TNF$^{-/-}$ BMMC-reconstituted Kit$^{W/W\text{-}v}$ mice (white triangles), and IL6$^{-/-}$ BMMC-reconstituted Kit$^{W/W\text{-}v}$ mice (white lozenges) at the indicated time points after intradermal injection with herpes simplex virus 2 (HSV-2; 7.5×10^4 PFU) are shown. TNF, tumor necrosis factor. $^*P<0.05$ and $^{**}P<0.01$ versus C57BL/6-Kit$^{W/W\text{-}v}$ mice. Data are representative of three independent experiments; $n = 10$ mice/group.

we conclude that enhanced TNF-α and IL-6 production in MCs by supernatants from HSV-2-infected keratinocytes is, at least in part, mediated by IL-33 signaling.

MCs do not contribute to the induction of HSV-specific CD8$^+$ T cells

Previous studies revealed a significant role of CD8$^+$ T cells in controlling HSV infections (Simmons and Tscharke, 1992; Chew *et al.*, 2009). Recent studies in mice demonstrated that migrating dermal CD103$^+$ and langerin-expressing DCs are the major transporters of HSV antigens out of skin and, together with resident CD8$^+$ DCs, are the major antigen-presenting cells of HSV antigens to CD8$^+$ T cells in draining lymph nodes (DLNs) (Allan *et al.*, 2003; Bedoui *et al.*, 2009). Therefore, we assessed the number of HSV-gB-specific CD8$^+$ T cells by using tetramer staining, as well as CD8α$^+$ DCs and langerin$^+$ DCs, in DLNs of Kit$^{+/+}$ and Kit$^{W/W\text{-}v}$ mice after intradermal infection with HSV. The proportions of HSV-gB-specific CD8$^+$ T cells in the DLNs of HSV-infected Kit$^{+/+}$ and Kit$^{W/W\text{-}v}$ mice at 6 days after infection were significantly increased when compared with that of uninfected mice (Figure 5a). However, the numbers of HSV-gB-specific CD8$^+$ T cells in Kit$^{+/+}$ and Kit$^{W/W\text{-}v}$ mice were comparable (Figure 5b), suggesting that MCs are not essential for the generation of HSV-specific CD8$^+$ T cells in primary cutaneous HSV-2 infection. Consistent with these findings, there was no significant difference in the frequency of CD8α$^+$ DCs or langerin$^+$ DCs in DLNs of Kit$^{+/+}$ and Kit$^{W/W\text{-}v}$ mice at 2 or 5 days after infection, respectively (Figure 5c). Similarly, no significant difference was detected in the number of CD4$^+$ CD25$^+$ Foxp3$^+$ regulatory T cells found in DLNs (Figure 5d). These results suggest that the impaired clearance of HSV-2 at the infection site observed in Kit$^{W/W\text{-}v}$ mice (Figure 1e) may not be attributed to the impaired induction of HSV-specific cytotoxic T lymphocytes (CTLs).

DISCUSSION

In this study, we have identified previously unknown functions of skin MCs in host protection against HSV-2. The contribution of MCs to host defense against HSV, one of the most common viral infections in the world, had been less clear, probably because MCs are resistant to HSV-2 infection. Indeed, recent

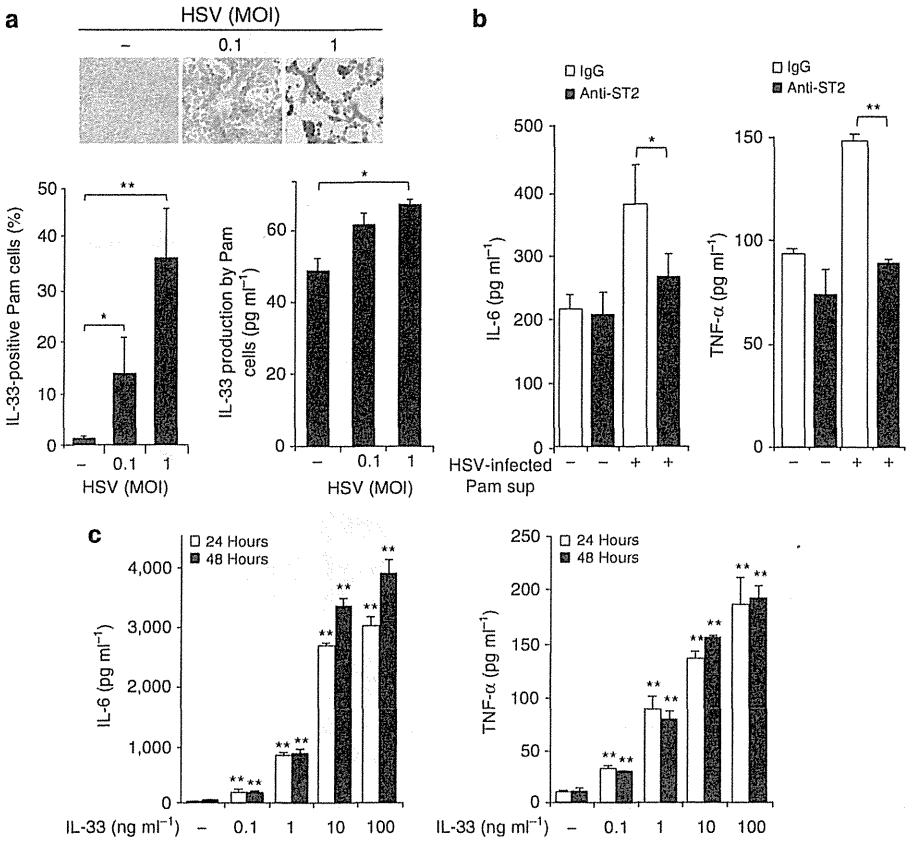

Figure 4. IL-33 is upregulated in herpes simplex virus 2 (HSV-2)–infected keratinocytes, and promotes IL-6 and tumor necrosis factor-α (TNF-α) production by mast cells (MCs). (**a**) Immunohistochemical staining for IL-33 in HSV-infected (multiplicities of infection (MOIs) 0.1 and 1) or uninfected Pam-212 cells 24 hours after infection (original magnification ×400). The percentage of IL-33-positive staining cells in the total population of Pam-212 cells was assessed throughout five high-power fields of view. IL-33 production by HSV-infected (MOIs 0.1 and 1) or uninfected Pam-212 cells 24 hours after infection. (**b**) Bone marrow–derived MCs (BMMCs) were pretreated with anti-T1/ST2 antibody or control IgG for 30 minutes, and then stimulated with culture supernatants (sup) from HSV-infected (MOI 30) or uninfected Pam-212 cells for 24 hours. (**c**) BMMCs were stimulated with control IgG (100 ng ml^{-1}), IL-33 (0.1–100 ng ml^{-1}), or lipopolysaccharide (LPS; 10 ng ml^{-1}) for 24 or 48 hours. (**b**, **c**) IL-6 and TNF-α production by BMMCs was assessed by ELISA. *P<0.05 and **P<0.01 versus results for control IgG. Data are representative of three independent experiments, showing the means (n = 3) ± SD.

studies have shown MC involvement in viral host defense, in which the infection of MCs with the virus, such as dengue virus or vaccina virus, is required for MC-mediated immune responses (St John *et al.*, 2011; Wang *et al.*, 2012). Unlike these viral infection models, we demonstrated that MCs are critically involved in viral host defense against HSV-2, even though relatively few HSV-2-infected MCs were detected *in vitro* and *in vivo* (Supplementary Figure S3a online and data not shown). We also report that MC deficiency resulted in impaired HSV-2 clearance at the infection sites during the first 72 hours after infection, suggesting that MCs have key roles as the first line of defense against HSV-2 rather than contributing to acquired immunity. Using "MC knock-in mouse" model, we also demonstrated the crucial contribution of MC-produced TNF-α and IL-6 to protective antiviral responses to HSV-2. Several previous studies suggested an antiviral mechanism involving TNF-α and IL-6 that is responsible for a direct reduction in viral replication or for increasing local infiltration of innate immune cells at the site of HSV infection (Feduchi *et al.*, 1989; Rossol-Voth *et al.*, 1991; Heise and Virgin, 1995; Lundberg *et al.*, 2007; Murphy *et al.*, 2008). In addition, the infiltrating cells, including plasmacytoid DCs, neutrophils, and NK cells, and their products including key antiviral cytokines IFN-α/β, may also provide other means of limiting HSV replication and eliminating virus-infected cells (Melchjorsen *et al.*, 2009).

A recent study revealed that MC-dependent CTL responses are important for an optimized host defense, such as protection against intracellular bacteria, because MCs can internalize, process, and present bacterial antigens and induce antigen-specific activation and proliferation of CD8$^+$ T cells upon infection with *Listeria monocytogenes* (Stelekati *et al.*, 2009). In our model of cutaneous HSV-2 infection, however, HSV-specific CTL generation in MC-deficient mice was not impaired. It is possible that differences in pathogens or their infection levels in MCs might explain the differences in MC

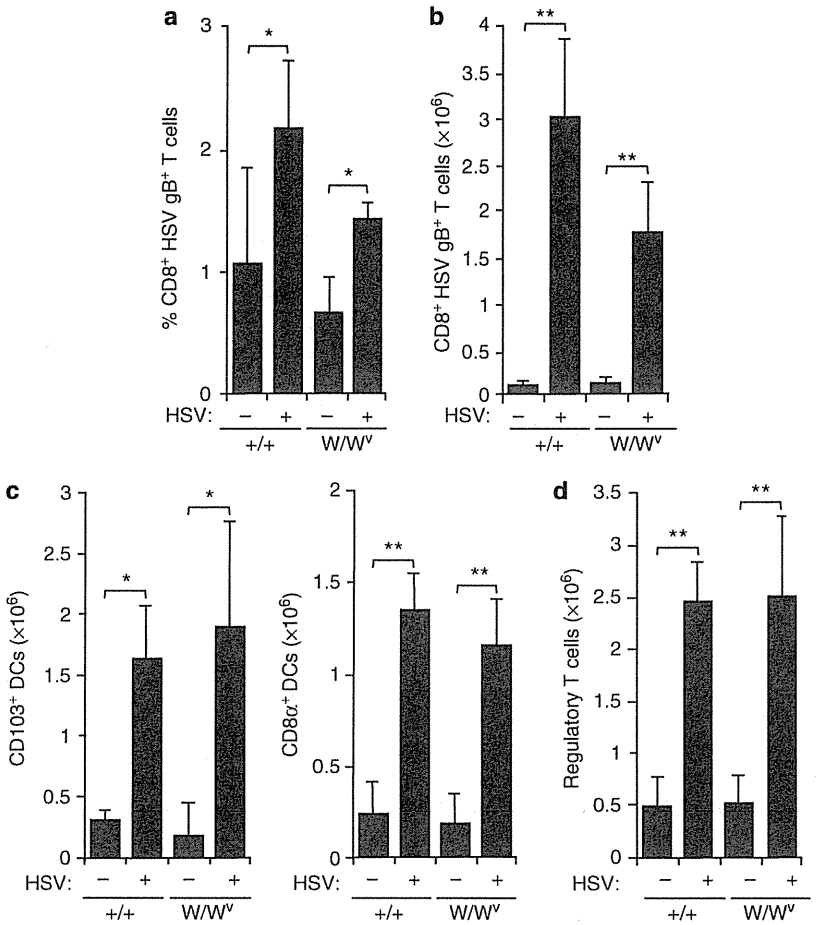

Figure 5. Mast cells (MCs) are not essential for the generation of herpes simplex virus 2 (HSV)–specific CD8$^+$ T cells. Kit$^{W/W\text{-}v}$ and Kit$^{+/+}$ mice were injected with HSV-2, as described in Figure 1. Draining lymph nodes (DLNs) were harvested at (**a**, **b**) 6, (**c**) 2 or 5, and (**d**) 3 days after infection. (**a**) The percentages of CD8$^+$ HSV gB$^+$ T cells in DLNs of HSV-2-infected and -uninfected mice were analyzed by flow cytometry using major histocompatibility complex (MHC) class I tetramer specific for HSV peptide glycoprotein B (gB) or tyrosinase-related protein 2 (TRP2) as a negative control (data not shown). (**b**) The number of CD8$^+$ HSV gB$^+$ T cells in DLNs. (**c**) The number of CD103$^+$ CD205$^+$ dendritic cells (DCs) at 5 days after infection and CD8α$^+$ DCs at 2 days after infection in DLNs. (**d**) The number of CD4$^+$ CD25$^+$ Foxp3$^+$ regulatory T-cell population in DLNs. $^*P<0.05$ and $^{**}P<0.01$ versus the corresponding uninfected mice. Data are representative of two independent experiments, showing the means ($n=5$ mice/group) ± SD.

contribution for CTL generation among these infection models. Nevertheless, in our model, it is still possible that MCs are involved in the recruitment of CTLs to the sites of HSV infection, because CD8$^+$ T-cell recruitment to sites of infection is facilitated by MCs during infection with Newcastle disease virus (Orinska *et al.*, 2005). Further detailed analysis under different viral infection is needed to reveal the functions and significance of MCs for CTL responses against viral infection.

The results of our study show that IL-33 derived from epidermal keratinocytes damaged by viral infection has a critical role in triggering the production of inflammatory cytokines by MCs. Although several viruses have been shown to infect and/or activate MCs *in vitro*, we observe neither significant HSV-2 infection nor HSV-induced direct activation of BMMCs monitored by cytokine production and degranulation. In contrast, the culture supernatants from HSV-2-treated keratinocytes, as well as IL-33 alone, induced TNF-α and IL-6 production by MCs independent of degranulation. The effect of the supernatants from HSV-2-treated keratinocytes was reduced consistently and most effectively by blockade of IL-33–IL-33R signaling in MCs. In addition, although we have recently reported that extracellular adenosine 5′-triphosphate also mediates "danger signal" derived from the damaged keratinocytes (Kawamura *et al.*, 2012), hydrolyzing extracellular adenosine 5′-triphosphate contained in the supernatants by soluble ecto-nucleoside triphosphate diphosphohydrolase (NTPDase; apyrase) did not affect TNF-α and IL-6 production by MCs (data not shown). These results clearly indicate the importance of IL-33 as an "alarmin" in cutaneous HSV infection. Our findings also suggest that IL-33 may be important for other cutaneous virus infections, such as varicella, hand–foot–mouse disease, warts, molluscum, and so on, which also induce the damage or degeneration of

keratinocytes. Further studies are needed to determine whether there is a significant *in vivo* role for IL-33 as an "alarmin" in viral infections other than HSV-2.

MATERIALS AND METHODS

Mice

Female c-Kit-mutant genetically MC-deficient C57BL/6-Kit$^{W/W\text{-}v}$ (Kit$^{W/W\text{-}v}$) mice and the congenic normal C57BL/6-Kit$^{+/+}$ (Kit$^{+/+}$) mice were purchased from Japan SLC (Hamamatsu, Japan). C57BL/6-Kit$^{W\text{-}sh/W\text{-}sh}$ (Kit$^{W\text{-}sh/W\text{-}sh}$) mice were obtained from Sankyo Labo Service (Tokyo, Japan). C57BL/6-Tnf$^{-/-}$ mice and C57BL/6-IL-6$^{-/-}$ mice were purchased from The Jackson Laboratory (Bar Harbor, ME). All animal experiments were carried out in strict accordance with the recommendations in Guidelines for Proper Conduct of Animal Experiments of Science Council of Japan. The protocol was approved by University of Yamanashi Animal Care and Use Committee (permit number: 19–50).

Virus

The WT HSV-2 strain 186 was prepared in Vero cells as described previously (Ushijima *et al.*, 2009), and stored at −80 °C with an approximate titer of 1×10^7 PFU per ml.

HSV inoculation of mice

Kit$^{+/+}$ mice, Kit$^{W/W\text{-}v}$ mice, and Kit$^{W\text{-}sh/W\text{-}sh}$ mice were injected intradermally with HSV-2 (7.5×10^4–7.5×10^5 PFU in 50 μl of EMEM; Nissui, Tokyo, Japan) on the right lower flank after shaving under diethyl ether anesthesia. Mice were then monitored for survival and scored for skin lesions and paralysis. Clinical score was assessed using the experimental autoimmune encephalomyelitis score, and skin lesions were scored as described previously (Takasaki *et al.*, 2000).

Measurement of viral titers and cytokines in HSV-2-inoculated skin

Kit$^{W/W\text{-}v}$ mice or Kit$^{+/+}$ mice were intradermally infected with 7.5×10^4 PFU of HSV-2 186 strain ($n = 3$) on the right back. The primary inoculation site of skin (8 × 8 mm) was excised at 1, 3, 5, or 7 days after infection, respectively. Skin samples were thawed and homogenized in 2 ml of Dulbecco's phosphate-buffered saline (Invitrogen, Carlsbad, CA) containing protease inhibitors (Thermo Scientific, Waltham, MA) with sea sand on ice, centrifuged at 7,000 r.p.m. for 5 minutes, and the supernatants were added on Vero cell monolayers. After 24 hours, cultures were fixed with 5% formalin, stained with 0.05% crystal violet, and plaques were counted using a dissecting microscope. For measurement of cytokines, skin samples were excised and homogenized in 250 μl of Tper EDTA-free lysis buffer (Pierce) containing protease inhibitors (Thermo Scientific). Cytokine screening was performed in the supernatants using the Multi-Analyte ELISArray Kit (SABiosciences, Fredrick, MD) according to the manufacturer's instructions.

Preparations of BMMCs

BMMCs were prepared from B6 mice BM cell suspensions, as described previously (Matsushima *et al.*, 2004). Briefly, crude BM cells (4×10^5 cells per ml) were cultured in complete RPMI-1640 (Invitrogen) in the presence of murine recombinant IL-3 (10 ng ml^{-1}) and recombinant stem cell factor (10 ng ml^{-1}; PeproTech, Boston, MA). Nonadherent and loosely adherent cells were recovered twice a week, and further expanded in fresh medium for 4 to 6 weeks. The resulting MC preparations contained >95% CD45$^+$ CD117$^+$ cells.

In vitro HSV infection of BMMCs and keratinocytes

For HSV-2 infection of keratinocytes, 1×10^5 Pam-212 keratinocytes were exposed to HSV-2 strain 186 at an MOI of 0.1, 1, 10, or 30 for 1 hour and washed three times. At 24 hours after incubation, the culture supernatants were collected and passed through a filter (Minisart high flow, pore size 0.1 μm; Sartorius Stedim Biotech, Goettingen, Germany) to remove free virus. For HSV-2 infection of MCs, 2×10^5 BMMCs were infected for 1 hour with HSV-2 at an MOI of 0.1, 1, or 10. Following infection, cells were washed three times and then incubated for an additional 24 hours. In some experiments, BMMCs were stimulated with the culture supernatants from Pam-212 cells, treated with or without HSV for 1 hour, or were stimulated with lipopolysaccharide from *E. coli* serotype 0111:B4, containing <1% protein and <1% RNA (10–100 ng ml^{-1}, Sigma-Aldrich, St Louis, MO) for 24 hours, as control. In the blocking experiments, the culture supernatants from HSV-infected (MOI 30) Pam-212 cells were pretreated with 20 μg ml^{-1} of anti-IL-1α (R&D Systems, Minneapolis, MN), IFN-β (Abcam, Cambridge, UK), and thymic stromal lymphopoietin (R&D Systems) mAbs or isotype-matched control IgG mAbs (BD Pharmingen, San Diego, CA) for 15 minutes before addition to BMMCs. For blocking IL-33-mediated signals, BMMCs were preincubated with 40 μg ml^{-1} of anti-T1/ST2 mAb (MABioproducts, Walkerville, MD) or isotype control mAb for 30 minutes before addition of the culture supernatants from HSV-infected Pam-212 cells. BMMCs were stimulated for 6 hours with the supernatants, washed three times, and incubated in their growth medium for an additional 24 hours. In some experiments, BMMCs were stimulated with control IgG (100 ng ml^{-1}), recombinant IL-33 (0.1–100 ng ml^{-1}, R&D Systems), or lipopolysaccharide (10 ng ml) for 24 or 48 hours. The levels of IL-1α, IL-6, TNF-α, IFN-α, IL-12, and IL-17 in the culture supernatants were determined using an ELISA kit (BD Pharmingen and eBiosciences, San Diego, CA) or the Multi-Analyte ELISArray Kit (SABiosciences) according to the manufacturer's instructions.

Degranulation assay

Degranulation was assessed by β-hexosaminidase assay, as described previously (Matsushima *et al.*, 2004). Briefly, the supernatants were incubated with 2.5 mM *p*-nitrophenyl-*N*-acetyl β-D glucosaminide (Sigma-Aldrich) for 90 minutes. The reactions were terminated by 0.4 M glycine, and the colored products were measured using an ELISA plate reader (Molecular Devices, Sunnyvale, CA).

Local MC reconstitution in Kit$^{W/W\text{-}v}$ mice

Four-week-old Kit$^{W/W\text{-}v}$ mice were transfused by intradermal injection with 2×10^6 BMMCs in 50 μl of RPMI derived from Kit$^{+/+}$, Tnf$^{-/-}$, or Il-6$^{-/-}$ mice as previously described (Grimbaldeston *et al.*, 2007). At 9 weeks after intradermal transfer, the BMMC-reconstituted Kit$^{W/W\text{-}v}$ mice were used for experiments.

Flow cytometry

Cells were stained with allophycocyanin (APC)-labeled anti-CD3, FITC- or phycoerythrin (PE)-anti-CD8, APC-anti-CD11c, FITC-anti-CD205, and PE-anti-CD103 mAbs (10 μg ml^{-1}, Pharmingen, San Diego, CA) for 30 minutes at 4 °C and analyzed on a FACSCalibur

(Becton Dickinson, Franklin Lakes, NJ). For tetramer staining, inguinal and axillary lymph nodes at 6 days after infection were stained with PE-H-2K^b HSV-1gB498-505 (SSIEFARL) tetramer, or PE-H-2K^b TRP2 tetramer (5 μg ml^{-1}, MBL, Nagoya, Japan) as control, for 20 minutes at 4 °C. To detect regulatory T cells or HSV-2-infected BMMCs, cells were fixed and permeabilized with Cytofix/Cytoperm reagents (BD Biosciences-Pharmingen), and then stained with APC-anti-Foxp3 mAb using the Foxp3 Staining Set (eBioscience) or FITC-anti-HSV glycoprotein D mAb (Argene, Verniolle, France), respectively.

Immunohistochemistry

Skin tissues were collected from infected sites at 1, 3, or 5 days after HSV infection and fixed in formalin. Paraffin-embedded sections were dewaxed and rehydrated through graded concentrations of ethanol. Tissue sections were stained with hematoxylin–eosin. Otherwise, the sections were preincubated with 3% hydrogen peroxide in methanol for 10 minutes to inactive endogenous peroxidase. Sections were incubated with rabbit anti-HSV-2 polyclonal antibody or control rabbit Ig for 1 hour at room temperature using the Dako envision kit (Dako, Glostrup, Denmark). The sections were washed and incubated with a goat anti-rabbit Ig conjugated to peroxidase-labeled dextran polymer for 1 hour at room temperature. After wash, they were treated with the chromogenic indicator dye 3,3′-diaminobenzidine for 5 minutes, and then counterstained with Mayer's hematoxylin. For IL-33 staining, plated Pam-212 cells exposed to HSV for 24 hours were washed and stained with goat anti-mouse IL-33 polyclonal antibody (R&D Systems) at 10 μg ml^{-1} for 3 hours at room temperature using the Dako LSAB kit (Dako). Cells were incubated with biotinylated anti-goat secondary antibody, and then incubated with peroxidase-conjugated streptavidin for 30 minutes. After development with 3,3′-diaminobenzidine substrate, cells were counterstained with Mayer's hematoxylin.

Statistical analyses

The GraphPad Prism 5 software (GraphPad Software, La Jolla, CA) was used to determine the statistical significance of survival data. Log-rank test was used for comparison of survival curves. Other data were analyzed by Student's *t*-test.

CONFLICT OF INTEREST

The authors state no conflict of interest.

ACKNOWLEDGMENTS

We thank Kazutoshi Harada and Naotaka Shibagaki for their helpful discussions, Hajime Suto for Kit$^{W\text{-}sh/W\text{-}sh}$ mice, and Miyuki Ogino for technical assistance. These studies were supported in part by a grant from the Ministry of Education and Science of the Japanese Government (grant 10377541, http://kaken.nii.ac.jp). The funder had no role in study design, data collection and analysis, decision to publish, or preparation of the manuscript.

SUPPLEMENTARY MATERIAL

Supplementary material is linked to the online version of the paper at http://www.nature.com/jid

REFERENCES

Abraham SN, St John AL (2010) Mast cell-orchestrated immunity to pathogens. *Nat Rev Immunol* 10:440–52

Allan RS, Smith CM, Belz GT *et al.* (2003) Epidermal viral immunity induced by CD8alpha+ dendritic cells but not by Langerhans cells. *Science* 301:1925–8

Bedoui S, Whitney PG, Waithman J *et al.* (2009) Cross-presentation of viral and self antigens by skin-derived CD103+ dendritic cells. *Nat Immunol* 10:488–95

Bonilla WV, Frohlich A, Senn K *et al.* (2012) The alarmin interleukin-33 drives protective antiviral CD8 T cell responses. *Science* 335:984–9

Chang YJ, Kim HY, Albacker LA *et al.* (2011) Innate lymphoid cells mediate influenza-induced airway hyper-reactivity independently of adaptive immunity. *Nat Immunol* 12:631–8

Cheng H, Tumpey TM, Staats HF *et al.* (2000) Role of macrophages in restricting herpes simplex virus type 1 growth after ocular infection. *Invest Ophthalmol Vis Sci* 41:1402–9

Chew T, Taylor KE, Mossman KL (2009) Innate and adaptive immune responses to herpes simplex virus. *Viruses* 1:979–1002

Corey L, Spear PG (1986) Infections with herpes simplex viruses (1). *N Engl J Med* 314:686–91

Dawicki W, Marshall JS (2007) New and emerging roles for mast cells in host defence. *Curr Opin Immunol* 19:31–8

Echtenacher B, Mannel DN, Hultner L (1996) Critical protective role of mast cells in a model of acute septic peritonitis. *Nature* 381:75–7

Feduchi E, Alonso MA, Carrasco L (1989) Human gamma interferon and tumor necrosis factor exert a synergistic blockade on the replication of herpes simplex virus. *J Virol* 63:1354–9

Galli SJ, Kalesnikoff J, Grimbaldeston MA *et al.* (2005) Mast cells as "tunable" effector and immunoregulatory cells: recent advances. *Annu Rev Immunol* 23:749–86

Grimbaldeston MA, Nakae S, Kalesnikoff J *et al.* (2007) Mast cell-derived interleukin 10 limits skin pathology in contact dermatitis and chronic irradiation with ultraviolet B. *Nat Immunol* 8:1095–104

Heise MT, Virgin HWt (1995) The T-cell-independent role of gamma interferon and tumor necrosis factor alpha in macrophage activation during murine cytomegalovirus and herpes simplex virus infections. *J Virol* 69:904–9

Kawamura T, Ogawa Y, Nakamura Y *et al.* (2012) Severe dermatitis with loss of epidermal Langerhans cells in human and mouse zinc deficiency. *J Clin Invest* 122:722–32

Kulka M, Alexopoulou L, Flavell RA *et al.* (2004) Activation of mast cells by double-stranded RNA: evidence for activation through Toll-like receptor 3. *J Allergy Clin Immunol* 114:174–82

Looker KJ, Garnett GP, Schmid GP (2008) An estimate of the global prevalence and incidence of herpes simplex virus type 2 infection. *Bull World Health Organ* 86:805–12

Lundberg P, Welander PV, Edwards CK 3rd *et al.* (2007) Tumor necrosis factor (TNF) protects resistant C57BL/6 mice against herpes simplex virus-induced encephalitis independently of signaling via TNF receptor 1 or 2. *J Virol* 81:1451–60

Luthi AU, Cullen SP, McNeela EA *et al.* (2009) Suppression of interleukin-33 bioactivity through proteolysis by apoptotic caspases. *Immunity* 31: 84–98

Malaviya R, Ikeda T, Ross E *et al.* (1996) Mast cell modulation of neutrophil influx and bacterial clearance at sites of infection through TNF-alpha. *Nature* 381:77–80

Matsushima H, Yamada N, Matsue H *et al.* (2004) TLR3-, TLR7-, and TLR9-mediated production of proinflammatory cytokines and chemokines from murine connective tissue type skin-derived mast cells but not from bone marrow-derived mast cells. *J Immunol* 173:531–41

Melchjorsen J, Matikainen S, Paludan SR (2009) Activation and evasion of innate antiviral immunity by herpes simplex virus. *Viruses* 1:737–59

Metz M, Maurer M (2007) Mast cells–key effector cells in immune responses. *Trends Immunol* 28:234–41

Metz M, Siebenhaar F, Maurer M (2008) Mast cell functions in the innate skin immune system. *Immunobiology* 213:251–60

Moussion C, Ortega N, Girard JP (2008) The IL-1-like cytokine IL-33 is constitutively expressed in the nucleus of endothelial cells and epithelial cells in vivo: a novel 'alarmin'? *PLoS One* 3:e3331

Murphy EA, Davis JM, Brown AS *et al.* (2008) Effect of IL-6 deficiency on susceptibility to HSV-1 respiratory infection and intrinsic macrophage antiviral resistance. *J Interferon Cytokine Res* 28:589–95

Orinska Z, Bulanova E, Budagian V *et al.* (2005) TLR3-induced activation of mast cells modulates CD8+ T-cell recruitment. *Blood* 106:978–87

Rossol-Voth R, Rossol S, Schutt KH *et al.* (1991) In vivo protective effect of tumour necrosis factor alpha against experimental infection with herpes simplex virus type 1. *J Gen Virol* 72(Pt 1):143–7

Simmons A, Tscharke DC (1992) Anti-CD8 impairs clearance of herpes simplex virus from the nervous system: implications for the fate of virally infected neurons. *J Exp Med* 175:1337–44

Stelekati E, Bahri R, D'Orlando O *et al.* (2009) Mast cell-mediated antigen presentation regulates CD8+ T cell effector functions. *Immunity* 31: 665–76

St John AL, Rathore AP, Yap H *et al.* (2011) Immune surveillance by mast cells during dengue infection promotes natural killer (NK) and NKT-cell recruitment and viral clearance. *Proc Natl Acad Sci USA* 108:9190–5

Takasaki I, Andoh T, Shiraki K *et al.* (2000) Allodynia and hyperalgesia induced by herpes simplex virus type-1 infection in mice. *Pain* 86:95–101

Ushijima Y, Goshima F, Kimura H *et al.* (2009) Herpes simplex virus type 2 tegument protein UL56 relocalizes ubiquitin ligase Nedd4 and has a role in transport and/or release of virions. *Virol J* 6:168

Wang Z, Lai Y, Bernard JJ *et al.* (2012) Skin mast cells protect mice against vaccinia virus by triggering mast cell receptor S1PR2 and releasing antimicrobial peptides. *J Immunol* 188:345–57

Pediatr Surg Int (2013) 29:1147–1152
DOI 10.1007/s00383-013-3371-z

ORIGINAL ARTICLE

RASSF1A methylation indicates a poor prognosis in hepatoblastoma patients

Shohei Honda · Hisayuki Miyagi · Hiromu Suzuki · Masashi Minato · Masayuki Haruta · Yasuhiko Kaneko · Kanako C. Hatanaka · Eiso Hiyama · Takehiko Kamijo · Tadao Okada · Akinobu Taketomi

Published online: 30 August 2013

Abstract
Purpose The RAS association domain family protein 1 (RASSF1A) is known to be frequently inactivated by promoter hypermethylation in cancers. This study investigated the association of *RASSF1A* methylation with clinical outcomes in hepatoblastoma patients and whether it is correlated with the histological phenotype of hepatoblastoma tumors.
Methods Seventy-four hepatoblastoma tumors were obtained from patients enrolled in the Japanese study group for pediatric liver tumor protocol-2. From nine formalin-fixed, paraffin-embedded specimens, we extracted DNA by dissection under a light microscope. We examined the methylation status of the *RASSF1A* promoter region by bisulfite pyrosequencing.
Results Twenty-five (33.8 %) hepatoblastoma tumors were classified as having methylated *RASSF1A*. The *RASSF1A* methylation was significantly associated with metastatic tumors and a poor prognosis. Despite the complete resection, five pretreatment extent of disease II tumors showed recurrence or distant metastasis postoperatively. Among these cases, four tumors were found to show *RASSF1A* methylation. When compared to histologically different types of cell, *RASSF1A* methylation values in samples of the normal liver, fetal type, and embryonal type, were significantly elevated in ascending order.
Conclusions We confirmed that *RASSF1A* methylation is a significant prognostic indicator in hepatoblastomas, and it may become a promising molecular marker to stratify patients into appropriate risk groups.

Keywords Hepatoblastoma · *RASSF1A* methylation · Prognostic marker

Supported by Ministry of Health, Labour, and Welfare, Japan [Grant-in-Aid for Cancer Research (S. Honda.)].

S. Honda · H. Miyagi · M. Minato · T. Okada (✉) · A. Taketomi
Department of Gastroenterological Surgery I, Hokkaido University Graduate School of Medicine, Kita-ku, Kita 15, Nishi 7, Sapporo 060-8638, Japan
e-mail: okadata@med.hokudai.ac.jp

H. Suzuki
Department of Molecular Biology, Sapporo Medical University, Sapporo, Japan

M. Haruta · Y. Kaneko
Department of Cancer Diagnosis, Research Institute for Clinical Oncology, Saitama Cancer Center, Saitama, Japan

K. C. Hatanaka
Department of Surgical Pathology, Hokkaido University Hospital, Sapporo, Japan

E. Hiyama
Japanese Study Group for Pediatric Liver Tumor, Hiroshima, Japan

T. Kamijo
Department of Biochemistry and Molecular Carcinogenesis, Chiba Cancer Center Research Institute, Chiba, Japan

Introduction

Hepatoblastoma is the most common malignant neoplasm of the liver in children. Despite the progress of therapy, the mortality rate remains at 35–50 % in high-risk patients, such as those with extrahepatic tumors, macroscopic invasion of large vessels, or distant or lymph node metastases [1]. Complete surgical resection or liver transplantation and mainstream treatment with cytotoxic drugs are essential for achieving a favorable long-term outcome. To

improve the mortality of hepatoblastoma patients in advanced stages, innovative treatment and potent prognostic markers for better therapy planning are needed.

Histologically, hepatoblastoma tumors are classified as wholly epithelial, or mixed epithelial and mesenchymal types. In the wholly epithelial type, there are two major subtypes, the fetal subtype and the mixed fetal and embryonal subtype [2]. Fetal and embryonal components often develop in combination, that is, heterogeneity is present. The RAS association domain family protein 1 (RASSF1A) is known to be frequently inactivated by promoter hypermethylation in many adult and childhood cancers [3]. We previously reported that *RASSF1A* methylation was correlated with a poor outcome by multivariate analysis, and suggested that *RASSF1A* may be a promising molecular–genetic marker predicting the treatment outcome in hepatoblastoma patients [4]. The association between the histological type and *RASSF1A* methylation is ambiguous despite the fact that the histologic features are associated with different prognoses; a pure fetal histology is favorable and small cell undifferentiated and macrotrabecular histologies are unfavorable [1]. Therefore, the current study was undertaken to determine the association with histological types by examining each type of hepatoblastoma cell dissected separately.

In this study, we investigated the methylation status of *RASSF1A* in hepatoblastoma tumors by bisulfite pyrosequencing, which is a rapid and accurate method to quantify DNA methylation. We analyzed the results with regard to patients' clinicopathological characteristics and prognosis, and evaluated its association with the histological phenotype on the basis of the epigenetic alteration of hepatoblastomas.

Methods

Patients and samples

Seventy-four hepatoblastoma patients with a median age of 18 months underwent tumor resection and partial hepatectomy between December 1999 and December 2008 at the institutions of the Japanese Study Group for Pediatric liver Tumors (JPLT). All patients were treated in the JPLT-2 study [5]. The extent of disease was determined at the time of initial biopsy or resection according to the classification of the pretreatment extent of disease (PRETEXT) staging system [6]. Metastatic tumors were found in 15 % of the patients (Table 1). The 5-year overall survival and event-free survival rates were 86.7 and 73.4 % for the 74 patients, respectively.

The DNA samples of the 74 hepatoblastoma tumors were supplied by JPLT, and they were extracted from fresh-frozen specimens. Furthermore, formalin-fixed, paraffin-embedded (FFPE) specimens were obtained from nine patients referred to our institution for surgical treatment between 1995 and 2011. We extracted DNA from different types of cell: fetal type, embryonal type, and normal liver, by dissection under a light microscope in order to avoid contamination with normal tissues and mesenchymal components. The ethics committee of our institution approved the study protocol, and signed

Table 1 Clinicopathological factors and *RASSF1A* methylation status in 74 patients with hepatoblastoma

Clinicopathological factors		No. of patients	*RASSF1A*		p value[1]
			Methylated	Unmethylated	
Sex	Male	45	14	31	0.360
	Female	29	11	18	
Age at diagnosis	<365 days	22	0	22	0.000064
	≥365 days	52	25	27	
PRETEXT	I	5	1	4	0.319
	II	27	7	20	
	III	29	10	19	
	IV	13	7	6	
Metastasis	No	63	15	48	0.000039
	Yes	11	10	1	
Histological type	Fetal	28	9	19	0.508
	Mixed fetal and embryonal	40	14	26	
	Unknown	6			
Outcome	Alive	63	15	48	0.000039
	Dead	11	10	1	

[1] Fisher's exact test

informed consent was obtained in all cases by local physicians of the participating institutions.

Evaluation of *RASSF1A* methylation level

We examined the methylation status of the *RASSF1A* promoter region by bisulfite pyrosequencing, which can calculate the level of methylation at each CpG site in samples after bisulfite treatment. Genomic DNA (500 ng) was modified with sodium bisulfite using an EpiTect bisulfite kit (Qiagen, Netherlands). Bisulfite pyrosequencing was carried out as described previously [7]. After PCR, the biotinylated PCR product was purified, made single-stranded, and used as a template in the pyrosequencing reaction. Briefly, the PCR products were bound to streptavidin sepharose beads HP (Amersham Biosciences, USA), after which beads containing the immobilized PCR product were purified, washed, and denatured using a 0.2 mol/L NaOH solution. After the addition of 0.3 μmol/L sequencing primer to the purified PCR product, pyrosequencing was carried out using a PSQ96MA system (Biotaga) and Pyro Q-CpG software (Biotage). The mean value of the methylation levels at two CpG sites in the *RASSF1A* promoter region was calculated. Primer sequences used in this study were as follows: forward, GAAGGAGGGAAGGAAGGGTAAG; reverse, GCCTCC CCCAAAATCCAA; sequencing primer, TTGTATTTAG GTTTTTATTG.

Statistical analysis

Correlations between the *RASSF1A* methylation status and clinicopathological factors were analyzed using the Fisher's exact test. Survival curves were constructed according to the methods of Kaplan and Meier, and comparisons of survival curves were performed with a log-rank test. One-way ANOVA followed by Student's *t* test with Bonferroni correction was used to compare methylation values of histologically different types of cell. A P value <0.05 was considered statistically significant.

Results

RASSF1A methylation status in 74 hepatoblastomas

The average of the *RASSF1A* methylation values in 74 hepatoblastoma tumors was 25.8 % (2.0–74.8 %). We performed the ROC analysis to determine the cutoff value of the *RASSF1A* methylation and adopted a cutoff value of 36.2 % in this study (Fig. 1). On the basis of this cutoff value, 25 (33.8 %) tumors were classified as having methylated *RASSF1A*, and the sensitivity and specificity for the patients having an event postoperatively were 77.8 and 80.4 %, respectively. There was only one patient who died in those with tumors with *RASSF1A* unmethylated (Fig. 2).

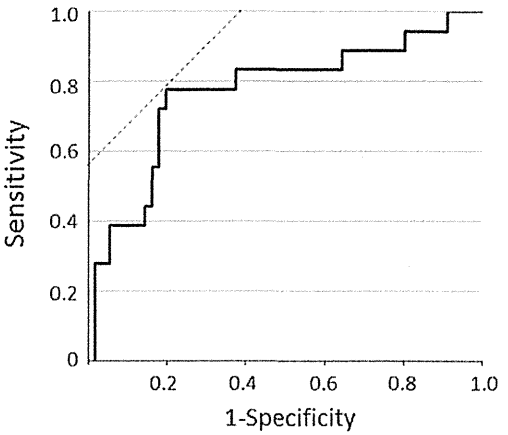

Fig. 1 ROC analysis to determine the cutoff value of the *RASSF1A* methylation

Associations between clinicopathological factors and *RASSF1A* methylation status

We evaluated the associations between the clinicopathological factors and *RASSF1A* methylation status in 74 patients. As Table 1 shows, there were no patients aged under 1 year who had a tumor with *RASSF1A* methylated; however, about half of the patients aged over 1 year were found to have a tumor with *RASSF1A* methylated. 10 of 25 patients (40 %) with a tumor with *RASSF1A* methylated suffered from metastatic tumors, although there was only one patient with metastasis in those with a tumor with *RASSF1A* unmethylated. This demonstrated that age at diagnosis and metastatic tumors were significantly associated with *RASSF1A* methylation. In Kaplan–Meier analyses, the patients with a tumor with methylated *RASSF1A* were significantly associated with a poor outcome: the 5-year overall survival and event-free survival rates were 63.6 and 35.5 %, respectively (Fig. 3).

The *RASSF1A* methylation was detected in 1 of 5 PRETEXT I tumors and 7 of 27 PRETEXT II tumors (Table 1). Despite complete resection, five PRETEXT II tumors showed recurrence or distant metastasis postoperatively, and three patients died. Among these cases, four tumors were found to have *RASSF1A* methylated.

Associations between histological types and *RASSF1A* methylation status

Next, we evaluated whether *RASSF1A* methylation is associated with the histopathological subtypes. Four of the

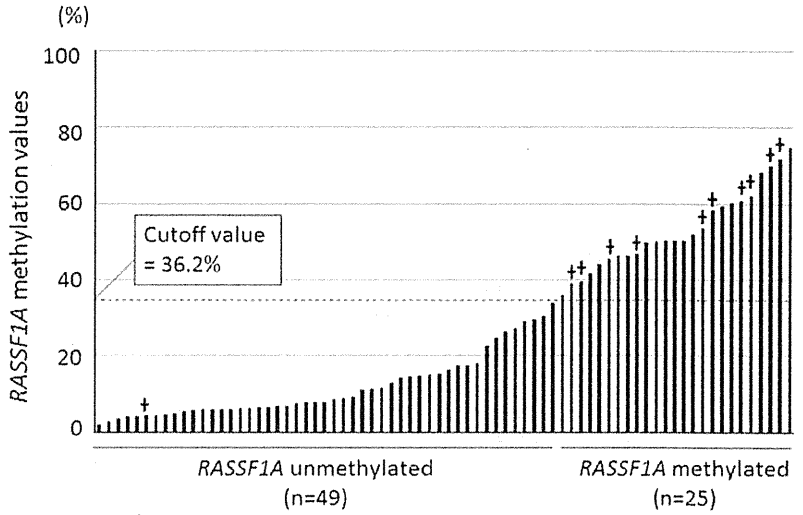

Fig. 2 *RASSF1A* methylation values in 74 patients with hepatoblastoma. *Plus* indicates the patient who died of the disease

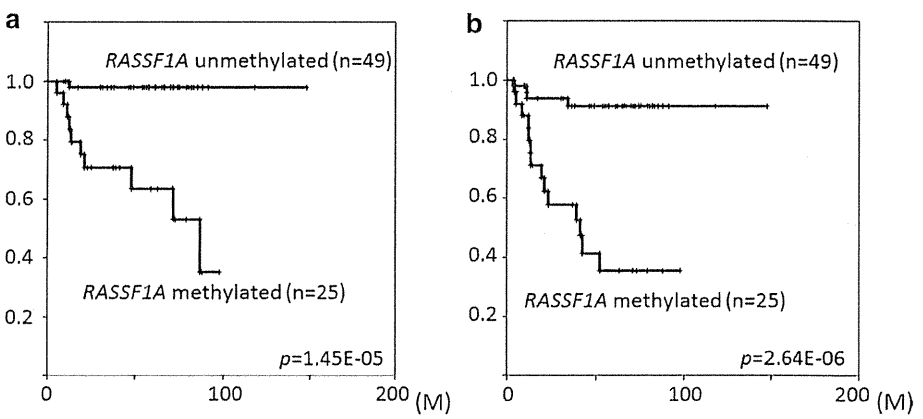

Fig. 3 **a** Overall survival curves and **b** event-free survival curves for hepatoblastoma patients classified by the methylation status of *RASSF1A*

nine tumors in FFPE specimens were classified pathologically into the mixed fetal and embryonal subtype, and DNA was extracted from the tumor cells of each subtype and the normal liver. The other five tumors were the pure fetal subtype, so DNA was extracted from fetal hepatoblastoma and normal liver cells.

The mean methylation values of *RASSF1A* in nine normal liver, nine fetal type, and four embryonal type samples were 8.6, 19.7, and 42.2 %, respectively (Fig. 4). This showed that fetal and embryonal types were significantly associated with *RASSF1A* methylation. Moreover, *RASSF1A* methylation values in samples of the normal liver, fetal type, and embryonal type were elevated in ascending order, when compared to each type of cell taken from the same patient.

Discussion

Complete surgical resection and chemotherapy including cisplatin remains the mainstay of hepatoblastoma treatment. In contrast to standard-risk patients, of who over 90 % achieve long-term survival, the treatment of patients with unrespectable and metastatic disease remains a challenge. Furthermore, there seems to exist a group of patients with high-risk tumors in PRETEXT II, which have a poorer prognosis despite the high-level resectability [5]. First, this study demonstrated that *RASSF1A* methylation was significantly associated with metastatic tumors and a poor prognosis, and that *RASSF1A* methylation may be useful to identify high-risk tumors in PRETEXT II. Secondly, *RASSF1A* methylation was also shown to be histologically correlated with different types of tumor. These findings suggest that *RASSF1A* may be a promising molecular marker to stratify the patients into appropriate risk groups in order to develop better therapeutic approaches.

The present factors predicting the outcome in hepatoblastoma patients include the age at diagnosis, histology, local growth pattern of the tumor, presence of metastasis, and the level of alpha–feto protein [1]. Chromosomal gains of 2q, 8q, and 20, high-level expression of *TERT* or *PLK1*, *CTNNB1* mutation, and *RASSF1A* methylation were shown

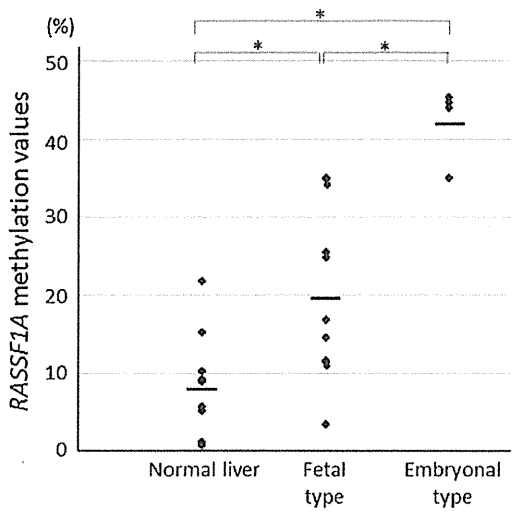

Fig. 4 *RASSF1A* methylation value for each sample is plotted by histological type. *Horizontal bars* indicate the mean value of each type. The p values were calculated by one-way ANOVA followed by Student's t test with Bonferroni correction ($^*p < 0.017$)

to be molecular–genetic markers predicting a poor outcome [4, 8, 9]. We have been focusing on *RASSF1A* methylation in hepatoblastomas, since it has been proven to be an independent prognostic factor by multivariate analysis [4]. RASSF1A inhibits tumor formation by apoptosis, and regulates microtubule dynamics and mitotic arrest via multiple effectors. By dysregulation of the Ras-signaling pathway, *RASSF1A* methylation is correlated with poor differentiation and vascular invasion of cancer cells, and an unfavorable outcome [10]. In child cancers, *RASSF1A* methylation was shown to be associated with a poor outcome in neuroblastoma and Wilms tumor [11, 12]. In this study, we newly adopted bisulfite pyrosequencing as a tool for methylation analysis because it is a highly effective and practical method and offers higher throughput compared to quantitative methylation-specific PCR used in the previous study [4]. We believe that bisulfite pyrosequencing can be a reliable tool when used in a clinical setting.

Cairo et al. [13] identified a 16-gene signature discriminating tumors with a fairly well-differentiated histology and a favorable prognosis against advanced and poorly differentiated tumors with a dismal outcome. In this study, *RASSF1A* methylation was also shown to be correlated with different types of histological phenotype by examining FFPE samples dissected separately. As shown in Table 1, there was no apparent difference in *RASSF1A* methylation values between the fetal subtype and the mixed fetal and embryonal subtype, probably because contamination with different types of tumor cell, normal tissues, and mesenchymal components could not be avoided using fresh-frozen specimens. With these gene signatures based on different phenotypes, the molecular classification of hepatoblastoma tumors may become possible after thorough clinical testing. Although the number of cases in this study is too small to draw definite conclusions, we expect that these molecular markers can be used as prognostic markers predicting the treatment outcome when larger clinical trials are carried out.

In conclusion, *RASSF1A* methylation was significantly associated with metastatic tumors and a poor prognosis in hepatoblastoma patients, and it may be especially useful to identify high-risk tumors in PRETEXT II. The *RASSF1A* methylation was also shown to be correlated with different histological phenotypes. We hope that this work will contribute to establishing a useful molecular marker to predict the outcome of hepatoblastoma patients, stratify the patients efficiently, and develop better therapeutic strategies.

Acknowledgments We would like to thank all the staff at institutes that participated in JPLT for enrolling their patients in the study. We are also grateful to JPLT steering committee members (Drs. T. Hishiki, K. Ida, K. Watanabe, S. Kondo, T. Oue, M. Yano, and T. Tajiri), JPLT pathological committee members (Drs. H. Horie, Y. Tanaka, and K. Inoue) and a data administrator for JPLT (Dr. K. Hiyama, Hiroshima University), for data managements and clinic-pathological review of these patients.

Conflict of interest The authors who have taken part in this study declare that they do not have anything to disclose regarding funding or any conflict of interest with respect to this manuscript. The first and the corresponding authors are JSPS members, and this abstract was selected for presentation at the 50th Annual Meeting of the Japanese Society of Pediatric Surgeons.

References

1. von Schweinitz D (2012) Hepatoblastoma: recent developments in research and treatment. Semin Pediatr Surg 21:21–30
2. Zimmermann A, Lopez-Terrada D (2011) Pathology of pediatric liver tumors. In: Zimmermann A, Perilongo G, Malogolowkin M, von Schweinitz D (eds) Pediatric liver tumors. Springer, Heidelberg, pp 83–112
3. Agathanggelou A, Cooper NC, Latif F et al (2005) Role of the Ras-association domain family 1 tumor suppressor gene in human cancers. Cancer Res 65:3497–3508
4. Honda S, Haruta M, Sugawara W et al (2008) The methylation status of RASSF1A promoter predicts responsiveness to chemotherapy and eventual cure in hepatoblastoma patients. Int J Cancer 123:1117–1125
5. Hishiki T, Matsunaga T, Sasaki F et al (2011) Outcome of hepatoblastomas treated using the Japanese study group for pediatric liver tumor (JPLT) protocol-2: report from the JPLT. Pediatr Surg Int 27:1–8
6. Brown J, Perilongo G, Shafford E et al (2000) Pretreatment prognostic factors for children with hepatoblastoma- results from the International society of paediatric oncology (SIOP) study SIOPEL 1. Eur J Cancer 36:1418–1425

7. Yang AS, Estécio MR, Doshi K et al (2004) A simple method for estimating global DNA methylation using bisulfite PCR of repetitive DNA elements. Nucleic Acids Res 32:e38
8. Ueda Y, Hiyama E, Kamimatsuse A et al (2011) Wnt signaling and telomerase activation of hepatoblastoma: correlation with chemosensitivity and surgical resectability. J Pediatr Surg 46:2221–2227
9. Yamada S, Ohira M, Horie H et al (2004) Expression profiling and differential screening between hepatoblastomas and the corresponding normal livers: identification of high expression of the PLK1 oncogene as a poor-prognostic indicator of hepatoblastomas. Oncogene 23:5901–5911
10. Agathanggelou A, Cooper WN, Latif F (2005) Role of the Ras-association domain family 1 tumor suppressor gene in human cancers. Cancer Res 65:3497–3508
11. Yang Q, Zage P, Kagan D et al (2004) Association of epigenetic inactivation of RASSF1A with poor outcome in human neuroblastoma. Clin Cancer Res 10:8493–8500
12. Ohshima J, Haruta M, Fujiwara Y et al (2012) Methylation of the RASSF1A promoter is predictive of poor outcome among patients with Wilms tumor. Pediatr Blood Cancer 59:499–505
13. Cairo S, Armengol C, De Reyniès A et al (2008) Hepatic stem-like phenotype and interplay of Wnt/beta-catenin and Myc signaling in aggressive childhood liver cancer. Cancer Cell 14:471–484

WORLD JOURNAL OF SURGICAL ONCOLOGY

RESEARCH Open Access

Surgical management of hepatocellular carcinoma with tumor thrombi in the inferior vena cava or right atrium

Kenji Wakayama[†], Toshiya Kamiyama[*†], Hideki Yokoo[†], Tatsuhiko Kakisaka[†], Hirofumi Kamachi[†], Yosuke Tsuruga[†], Kazuaki Nakanishi[†], Tsuyoshi Shimamura[†], Satoru Todo[†] and Akinobu Taketomi[†]

Abstract

Background: The prognosis for advanced hepatocellular carcinoma (HCC) with tumor thrombi in the inferior vena cava (IVC) or right atrium (RA) is poor, and there is no established effective treatment for this condition. Thus study aimed to evaluate the efficacy of surgical resection and prognosis after surgery for such cases.

Methods: Between January 1990 and December 2012, 891 patients underwent hepatectomy for HCC at our institution. Of these, 13 patients (1.5%) diagnosed with advanced HCC with tumor thrombi in the IVC or RA underwent hepatectomy and thrombectomy. Data detailing the surgical outcome were evaluated and recurrence-free and overall survival rates were calculated using the Kaplan-Meier method.

Results: Seven patients had an IVC thrombus and six had an RA thrombus. Extra-hepatic metastasis was diagnosed in 8 of 13 patients. Surgical procedures included three extended right lobectomies, three extended left lobectomies, five right lobectomies, and two sectionectomies. Right adrenal gland metastases were excised simultaneously in two patients. All IVC thrombi were removed under hepatic vascular exclusion and all RA thrombi were removed under cardiopulmonary bypass (CPB). Four patients (30.8%) experienced controllable postoperative complications, and there was no surgical mortality. The mean postoperative hospital stay for patients with IVC and RA thrombi was 23.6 ± 12.5 days and 21.2 ± 4.6 days, respectively. Curative resection was performed in 5 of 13 cases. The 1- and 3-year overall survival rates were 50.4%, and 21.0%, respectively, and the median survival duration was 15.3 months. The 1- and 3-year overall survival rates for patients who underwent curative surgical resection were 80.0% and 30.0%, respectively, with a median survival duration of 30.8 months. All patients who underwent curative resection developed postoperative recurrences, with a median recurrence-free survival duration of 3.8 months. The 1-year survival rate for patients who underwent noncurative surgery and had residual tumors was 29.2%, with a median survival duration of 10.5 months.

Conclusions: Aggressive surgical resection for HCC with tumor thrombi in the IVC or RA can be performed safely and may improve the prognoses of these patients. However, early recurrence and treatment for recurrent or metastatic tumors remain unresolved issues.

Keywords: Hepatocellular carcinoma, Inferior vena cava, Right atrium, Tumor thrombus, Surgery

* Correspondence: t-kamiya@med.hokudai.ac.jp
[†]Equal contributors
Department of Gastroenterological Surgery 1, Hokkaido University Graduate School of Medicine, N-15, W-7, Kita-ku, Sapporo, Japan

Background

Hepatocellular carcinoma (HCC) is a highly malignant tumor with a propensity for invading intrahepatic blood vessels such as the portal vein (PV) or hepatic vein in advanced stages [1]. Further extension of tumor thrombi from any of the three main hepatic veins or the right inferior hepatic vein can give rise to thrombi in the inferior vena cava (IVC) or right atrium (RA) [1-3]. Commonly, the prognosis of HCC patients presenting with IVC or RA thrombosis is extremely poor [4-6], and there is no established management for such cases [4,5,7-17]. Surgical removal of IVC and RA thrombi combined with hepatectomy is the only radical treatment to decrease the risk of systemic metastasis and sudden death due to pulmonary embolism or occlusion of the tricuspid valve with a tumor thrombus [18-20]. However, aggressive surgical resection is not common because the surgical approach to IVC and RA thrombi is considered complicated and hazardous and is applicable only in limited cases with good hepatic reserve [4,6,9,16,17]. Therefore, the efficacy of surgical treatment for HCC with IVC or RA thrombi remains unclear. In this study, we retrospectively investigated the surgical outcomes and prognoses of patients who underwent surgery for HCC with IVC or RA tumor thrombi in a single institution to clarify the safety and efficacy of surgical resection.

Methods

Patients and diagnoses

Between January 1990 and December 2012, 891 patients underwent hepatectomy for HCC at the Department of Gastroenterological Surgery, Hokkaido University, Japan. The diagnosis of HCC was determined by enhanced computed tomography (CT) and magnetic resonance imaging (MRI). IVC or RA thrombi were evaluated by CT (Figure 1). Among those studied, 13 patients (1.5%) diagnosed with advanced HCC and tumor thrombi in the IVC or RA underwent hepatectomy. This study was approved by the Institutional Review Board of the Hokkaido University School of Advanced Medicine.

The mean age at diagnosis was 63.4 years. The most common cause of HCC was hepatitis B virus (HBV) infection (53.8%), followed by hepatitis C virus (HCV) infection (15.4%). A total of 12 (92.3%) patients were male, and according to the Child-Pugh classification, all cases had Child-Pugh class-A disease. Six (46.2%) patients had a single tumor and seven (53.8%) had multiple tumors. The mean main tumor size was 11.8 cm, with nine tumors (69.2%) located in the right lobe and four (30.8%) in the left lobe. Extra-hepatic metastases were detected in eight of thirteen (61.5%) patients (five with lung, two with right adrenal gland and one with mediastinal lymph node metastases). Seven (53.8%) patients had an IVC thrombus and five (46.2%) had an RA thrombus (Table 1).

The tumor thrombus arose from the right hepatic vein in four patients (30.8%), middle hepatic vein in three (23.1%), left hepatic vein in one (7.7%), inferior right hepatic vein in two (15.4%), right hepatic vein combined with the middle hepatic vein in one (7.7%), and right hepatic vein combined with the inferior right hepatic vein in one (7.7%). In one patient with right adrenal gland metastasis, the tumor thrombus arose from the right adrenal vein (7.7%). Two patients had a mural thrombus and eleven had a massive thrombus. The massive thrombi in 10 patients did not completely occlude the IVC because circinate or arc-like luminal flow in the IVC around the tumor thrombi was present and the outflow canals of the intact hepatic veins were maintained. The tumor thrombus of one patient completely occluded the IVC inferior to the influx of hepatic veins accompanied by an aggregating blood thrombus. The outflow canals of the intact hepatic veins were severely narrowed but not completely occluded. One patient with a thrombus completely occluding the IVC and two patients with a massive IVC thrombus suffered preoperative renal insufficiency, and two had evident leg edema (Table 2).

Surgical procedures

A lobectomy was performed for patients with an indocyanine green retention rate at 15 minutes after injection (ICG R_{15}) of <15% and total bilirubin levels of <1.5 mg/dl without ascites. Patients with an ICG R_{15} of 15 to 20% and total bilirubin levels of 1.5 to 2.0 mg/dl were eligible for sectionectomy according to our criteria [21]. The type of surgical procedure was selected based on Couinaud's classification [22] and included three extended right hepatectomies, three extended left hepatectomies, five right hepatectomies, and two sectionectomies accompanied by thrombectomies. The right adrenal gland was resected simultaneously in two patients with right adrenal gland metastases (Table 3).

Hepatic resections were performed with an ultrasonic dissector using the Pringle maneuver in all cases. All IVC thrombi were removed under hepatic vascular exclusion (HVE). Before thrombectomy, hepatic transection was performed and the IVC was clamped below and above the liver. The IVC thrombus was excised en-bloc from the incised IVC, with satisfactory visualization of the intraluminal space under HVE. The IVC incision was closed by a simple continuous suture without a patch. All RA thrombi were removed under cardiopulmonary bypass (CPB). Following a laparotomy, a median sternotomy was performed to prepare for prompt CPB in anticipation of an undesirable pulmonary tumor embolism from a dislodged thrombus. Hepatic transection was then performed. The liver was handled gently, particularly if the thrombus had a long, thin neck, to

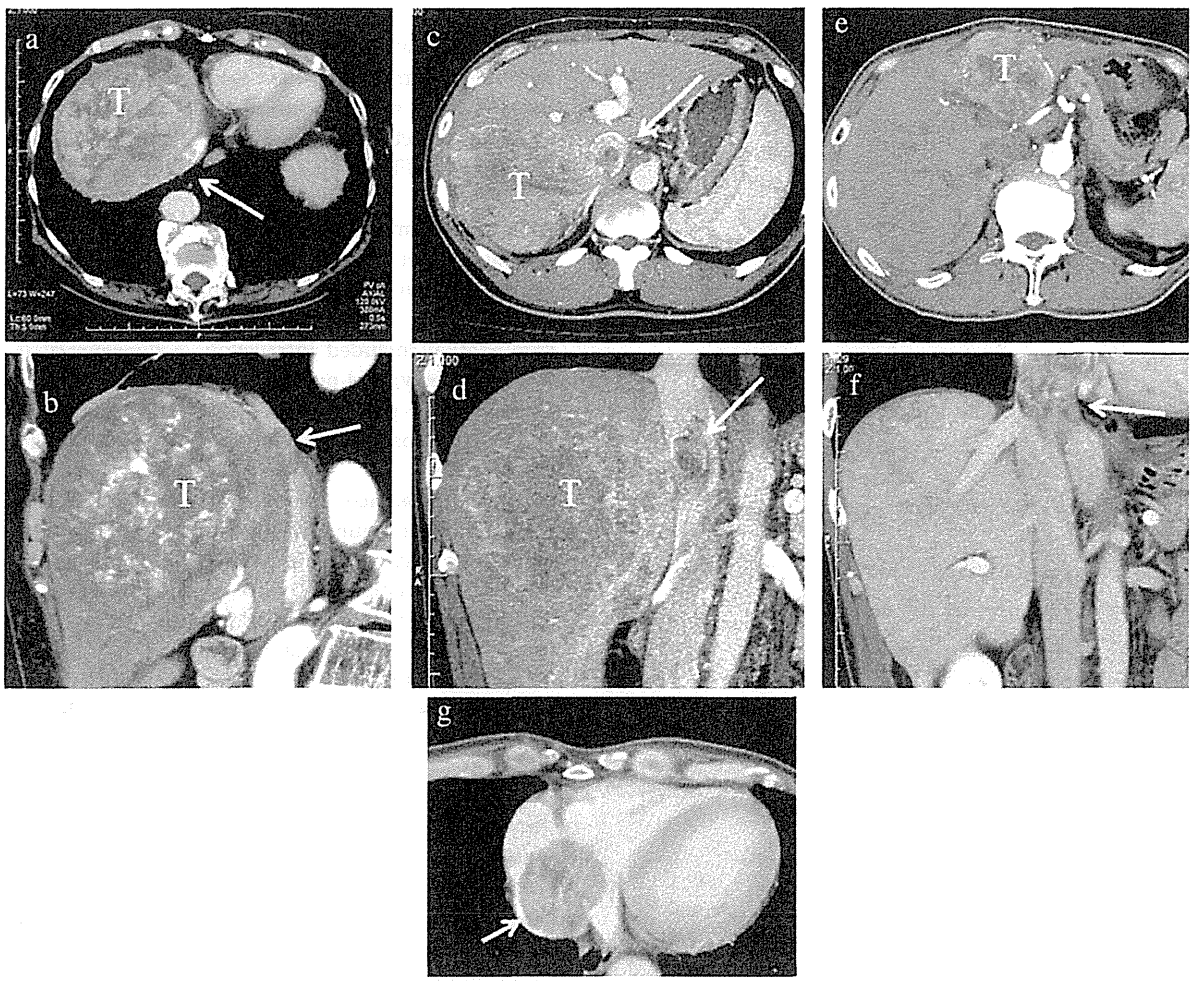

Figure 1 Representative computed tomography findings of hepatocellular carcinoma (HCC) with inferior vena cava (IVC) and right atrium (RA) thrombi. (**a** and **b**) A large HCC lesion in the right lobe (T), with a tumor thrombus arising from the right hepatic vein into the IVC (arrow). (**c** and **d**) HCC in the right lobe (T), with a tumor thrombus arising from the inferior right hepatic vein into the IVC (arrow). (**e**, **f**, and **g**) HCC in the left lobe (T), with a tumor thrombus arising from the left hepatic vein into the RA (arrow).

prevent dissemination of tumor thrombi. Then, the superior vena cava (SVC) and IVC below the liver were clamped and blood flow was bypassed to the ascending aorta via an oxygenator. The RA was incised and the thrombus was excised en-bloc under direct vision. In most cases, the RA was reconstructed by simple sutures, but in two cases, an invaded RA wall was partially excised and reconstructed using an artificial graft or pericardial patch. In addition to CPB, one patient with complete IVC occlusion accompanied by severe obstruction of intact hepatic outflow and one patient with tumor thrombi that arose from two major hepatic veins showed gross hepatic congestion due to outflow block at surgery. These cases needed extracorporeal bypass from the portal vein (PV) and IVC to SVC (Table 3). In all cases, thrombi were intraoperatively monitored by transesophageal echocardiography. In this study, we defined curative resection as macroscopic complete excision of the tumors, including metastatic lesions.

Follow up

The median duration of follow up was 11.2 (range, 1.8 to 51.8) months. Hospital death was defined as death occurring within 30 days of the first hospitalization. After surgery, CT or MRI was performed at 1- to 3-month intervals to determine recurrence. Data on surgical outcomes, postoperative management, recurrence, treatment of recurrence, and survival was analyzed for all cases.

Statistical analysis

Survival rates were analyzed by the Kaplan-Meier method and statistical significance was determined by

Table 1 Characteristics of patients and tumors

Characteristic	Value
Total number of patients	13
Age, years	
Mean ± SD (range)	63.4 ± 11.8 (37 to 86)
Sex	
Male/female	12/1
Hepatitis B virus	
Positive/negative	7/6
Hepatitis C virus	
Positive/negative	2/11
Child-Pugh classification	
A/B/C	13/0/0
Main tumor location	
Anterior/posterior/median/lateral section	5/4/3/1
Tumor size, cm	
Mean ± SD (range)	11.8 ± 4.3 (3.5–19)
Number of tumors	
Single/multiple	6/7
Extension of thrombus	
Inferior vena cava/right atrium	7/6
Preoperative extrahepatic metastases	
None/lung/adrenal gland/lymph nodes	5/5/2/1
Status of metastases after surgery	
Resected/regressed or stationary/progressed	3/1/4
Postoperative metastatic recurrence	
Liver/lung/lymph node/adrenal gland/inferior vena cava/brain	8/7/4/2/2/2

the log-rank test using JMP Pro 10.0.0 software (SAS, Cary, NC, USA). Significance was defined as $P < 0.05$.

Results

Surgical outcomes and postoperative complications

With regard to patients with an IVC thrombus, the mean surgical duration was 349 ± 30 minutes, the median blood loss was 950 ± 100 ml, and the mean HVE duration was 8.8 ± 3.1 minutes. Two of seven (28.6%) patients needed blood transfusions. No patient required an ICU stay, and the mean postoperative hospital stay was 23.6 ± 12.5 days. After surgery, one patient experienced biloma and one experienced controllable ascites. With regard to patients with an RA thrombus, the mean surgical duration was 608 ± 169 minutes, the median blood loss was 6540 ± 5404 ml, and the mean CPB duration was 32.2 ± 18.3 minutes. Five of six (83.3%) patients needed blood transfusions. The mean postoperative ICU stay was 1.7 ± 0.8 days and the mean postoperative hospital stay was 21.2 ± 4.6 days. After surgery, one patient experienced acute renal failure and one experienced atrial fibrillation, but these patients recovered with medical therapy. There was no postoperative mortality. All IVC and RA thrombi were excised completely. Curative resection was performed in five of thirteen (38.5%) cases (Table 4).

Postoperative management

Among the five patients (38.5%) who underwent curative resection, adjuvant systemic chemotherapy was administered to four. The chemotherapeutic agents used in combination included intravenous 5-fluorouracil (5-FU; 500 mg weekly) and peroral tegafur uracil (UFT; 300 mg daily) in three patients and peroral UFT (300 mg daily) in one. One patient was followed up without adjuvant chemotherapy.

Tumors remained after surgery in eight (61.5%) patients, including lung metastases in four, intrahepatic metastases in two, both intrahepatic and lung metastases in one, and mediastinal lymph node metastases in one. Residual lung metastases were treated with oral administration of UFT in two patients, 5-FU + UFT in one patient, and oral administration of tegafur gimeracil oteracil potassium (S-1) followed by surgical resection in one patient. Unresectable intrahepatic metastases were treated with UFT in two patients and transarterial chemoembolization (TACE) in one patient. A patient with residual mediastinal lymph node metastasis received radiation after surgery.

Recurrence and survival

All five patients who underwent curative resection experienced postoperative recurrences. Intrahepatic recurrences appeared in all five patients, lung metastases in four, intra-IVC metastases in one, and left adrenal gland metastases in one patient. The median recurrence-free survival duration of the patients who underwent curative resection was 3.8 months. Intrahepatic recurrences were treated with TACE in three patients, radiofrequency ablation (RFA) in two, and radiotherapy in one patient. Lung metastases were treated with systemic chemotherapy in three patients (5-FU + UFT in two, cisplatin (CDDP) + S-1 followed by oral administration of sorafenib in one patient), and surgical resection in one patient. Left adrenal gland metastases were surgically excised.

Among the eight patients who underwent noncurative resection, four of five with lung metastases exhibited progression of the metastases. In one patient, lung metastasis was resected but recurred after resection. Intrahepatic residual tumors in three patients progressed after surgery; however, mediastinal lymph node metastases treated by irradiation remained unchanged. Among these eight patients, seven experienced further dissemination of the tumor to new locations, including the lung in three, lymph